

## (10,3)-a Noninterpenetrated Network Built from a Piedfort Ligand Pair

Yanxiong Ke, David J. Collins, Daofeng Sun, and Hong-Cai Zhou\*

Department of Chemistry and Biochemistry, Miami University, Oxford, Ohio 45056

Received November 2, 2005

The Friedel–Crafts reaction of cyameluric chloride with toluene and subsequent oxidation have resulted in the synthesis of a benzoic acid functionalized tri-*s*-triazine derivative, *s*-heptazine tribenzoate (HTB). Photoluminescence and mass spectroscopy data indicate that, in solution, HTB molecules interact by face-to-face  $\pi$ – $\pi$  stacking, forming dimers (the “Piedfort unit”). A porous metal–organic framework (MOF) with a (10,3)-a chiral network has been synthesized with these dimers at the three-connected nodes linking trinuclear zinc clusters. Within the network, the dimer can exist in either of two enantiomeric forms because of an angular offset in the stacking. The resulting MOF is neutral and noninterpenetrated and exhibits a high solvent-accessible volume (calculated 84%).

Porous solids with chiral structure attract special research interest because of their potential applications in asymmetric catalysis, chiral separation, and nonlinear optics.<sup>1</sup> The chiral (10,3)-a network is of great importance in the field of porous metal–organic frameworks (MOFs); this network can be predictably synthesized from three-connected organic bridging ligands and inorganic nodes. In the past decade, some (10,3)-a networks based on oxygen and nitrogen donors have been investigated.<sup>2</sup> Specifically, a rare example of a (10,3)-a network MOF with homochiral permanent microporosity, which showed enantioselective sorption, was reported recently.<sup>3</sup>

A number of factors determine the overall stability, porosity, and network configuration of an MOF. Increasing the size of the ligand can allow the formation of larger pores;

with larger ligands, there is also an increased likelihood of forming an interpenetrated network. Interpenetration can stabilize the structure of an MOF against decomposition due to solvent loss or heating but can drastically reduce the size of the pores.<sup>4</sup> Another method of stabilization of the network, which sacrifices less pore space, can come from increased interaction between ligands in the form of  $\pi$ – $\pi$  stacking.

While investigating new bridging ligands for porous MOFs in order to address the above considerations, we became interested in the derivatives of tri-*s*-triazine (1,3,4,6,7,9,9b-heptaazaphenylene, also called *s*-heptazine); such derivatives possess an ideal trigonal geometry for three-connected networks. Compounds based on tri-*s*-triazine can also be expected to have a number of intriguing properties. First, the tri-*s*-triazine ring has excellent thermal stability.<sup>5–7</sup> Second, all reported tri-*s*-triazine derivatives exhibit interesting optical properties.<sup>5–11</sup> Third, recent theoretical calculations have shown that tri-*s*-triazine derivatives should have interesting electronic structures,<sup>12</sup> including strong  $\pi$ – $\pi$  interaction between the heterocyclic tri-*s*-triazine rings, each of which contains 14 delocalized  $\pi$  electrons. In the related, more thoroughly investigated smaller *s*-triazine system, examples of ligand pairing with face-to-face  $\pi$ – $\pi$  stacking, nicknamed the “Piedfort unit”, have been reported.<sup>13,14</sup>

\* To whom correspondence should be addressed. E-mail: zhouh@muohio.edu.

- (1) (a) Seo, J. S.; Whang, D.; Lee, H.; Jun, S. I.; Oh, J.; Jeon, Y. J.; Kim, K. *Nature* **2000**, *404*, 982. (b) Verbiest, T.; Van Elshocht, S.; Karuanen, M.; Helleman, L.; Snauwaert, J.; Nuckolls, C.; Katz, T. J.; Persoons, A. *Science* **1998**, *282*, 913.
- (2) (a) Abrahams, B. F.; Batten, S. R.; Hamit, H.; Hoskins, B. F.; Robson, R. *Chem. Commun.* **1996**, 1313. (b) Abrahams, B. F.; Haywood, M. G.; Hudson, T. A.; Robson, R. *Angew. Chem., Int. Ed.* **2004**, *43*, 6157. (c) Abrahams, B. F.; Jackson, P. A.; Robson, R. *Angew. Chem., Int. Ed.* **1998**, *37*, 2656. (d) Carlucci, L.; Ciani, G.; Proserpio, D. M.; Sironi, A. *J. Am. Chem. Soc.* **1995**, *117*, 12861. (e) Carlucci, L.; Ciani, G.; Proserpio, D. M.; Sironi, A. *J. Am. Chem. Soc.* **1995**, *117*, 4562. (f) Eubank, J. F.; Walsh, R. D.; Eddaoudi, M. *Chem. Commun.* **2005**, 2095. (g) Yaghi, O. M.; Davis, C. E.; Li, G.; Li, H. *J. Am. Chem. Soc.* **1997**, *119*, 2861.
- (3) Bradshaw, D.; Prior, T. J.; Cussen, E. J.; Claridge, J. B.; Rosseinsky, M. *J. Am. Chem. Soc.* **2004**, *126*, 6106.

- (4) (a) Reineke, T. M.; Eddaoudi, M.; Moler, D.; O’Keeffe, M.; Yaghi, O. M. *J. Am. Chem. Soc.* **2000**, *122*, 4843. (b) Yaghi, O. M.; Li, H.; Davis, C.; Richardson, D.; Groy, T. L. *Acc. Chem. Res.* **1998**, *31*, 474.
- (5) Horvath-Bordon, E.; Kroke, E.; Svoboda, I.; Fuess, H.; Riedel, R. *New J. Chem.* **2005**, *29*, 693.
- (6) Horvath-Bordon, E.; Kroke, E.; Svoboda, I.; Fuess, H.; Riedel, R.; Neeraj, S.; Cheetham, A. K. *Dalton Trans.* **2004**, 3900.
- (7) Kroke, E.; Schwarz, M.; Horvath-Bordon, E.; Kroll, P.; Noll, B.; Norman, A. D. *New J. Chem.* **2002**, *26*, 508.
- (8) Juergens, B.; Irran, E.; Senker, J.; Kroll, P.; Mueller, H.; Schnick, W. *J. Am. Chem. Soc.* **2003**, *125*, 10288.
- (9) Rossman, M. A.; Leonard, N. J.; Urano, S.; LeBreton, P. R. *J. Am. Chem. Soc.* **1985**, *107*, 3884.
- (10) Miller, D. R.; Swenson, D. C.; Gillan, E. G. *J. Am. Chem. Soc.* **2004**, *126*, 5372.
- (11) Shahbaz, M.; Urano, S.; LeBreton, P. R.; Rossman, M. A.; Hosmane, R. S.; Leonard, N. J. *J. Am. Chem. Soc.* **1984**, *106*, 2805.
- (12) (a) Zheng, W.; Wong, N.-B.; Liang, X.; Long, X.; Tian, A. *J. Phys. Chem. A* **2004**, *108*, 840. (b) Zheng, W.; Wong, N.-B.; Wang, W.; Zhou, G.; Tian, A. *J. Phys. Chem. A* **2004**, *108*, 97. (c) Zheng, W.; Wong, N.-B.; Zhou, G.; Liang, X.; Li, J.; Tian, A. *New J. Chem.* **2004**, *28*, 275.
- (13) Jessiman, A. S.; MacNicol, D. D.; Mallinson, P. R.; Vallance, I. *Chem. Commun.* **1990**, 1619.

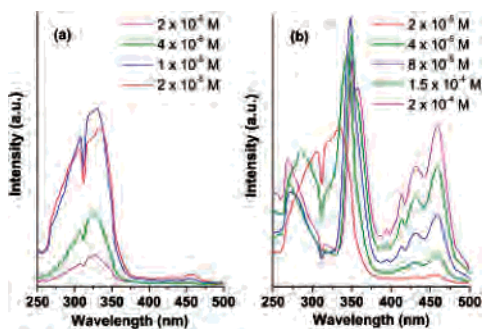


**Figure 1.** Photoluminescence excitation spectra of **2** at varying concentrations in DMF.

Herein, we report the synthesis of a novel triangular ligand based on tri-*s*-triazine, which we have designated as HTB (for *s*-heptazine tribenzoate). This ligand was designed with the above considerations in mind in order to take advantage of ligand dimerization; it was expected that HTB would exhibit Piedfort ligand pairs in solution and that these dimers would be incorporated into any MOF constructed using this ligand. As proof-of-concept, an MOF containing HTB is also reported. As expected, in contrast to frameworks built containing the common trifunctional carboxylate ligand 1,3,5-benzenetricarboxylic acid (BTC), the use of the HTB ligand resulted in a noninterpenetrated network; additionally, the resulting MOF was found to possess several desirable properties, namely, a (10,3)-a chiral network stabilized by ligand  $\pi$ - $\pi$  stacking and exhibiting a high solvent-accessible volume.

The synthesis of HTB is based on the Friedel–Crafts reaction of cyameluric chloride with toluene, yielding 2,5,8-tris(*p*-methylbenzene)-1,3,4,6,7,9,9b-heptaazaphenalene (**1**).<sup>15</sup> By selective oxidation of the methyl group into carboxylate, the benzoic acid functionalized ligand HTB was obtained [2,5,8-tris(*p*-benzoate)-1,3,4,6,7,9,9b-heptaazaphenalenic acid (**2**)].

To determine whether HTB molecules are paired in solution, preliminary studies on **1** and **2** were performed prior to their incorporation into the MOF  $\text{Zn}_3(\text{HTB})_2(\text{H}_2\text{O})_2 \cdot 3\text{DMA} \cdot 5\text{H}_2\text{O}$  (**3**). Because stacking and the formation of dimers is known to quench photoluminescence, the excitation spectra of **1** and **2** were examined. Mass spectroscopy was also employed on solutions of **1** and **2**.

The photoluminescence spectrum of **2** in a dimethylformamide (DMF) solution at varying concentrations was measured. A red shift in the emission was observed with increasing concentration, from 516 nm at a concentration of  $2 \times 10^{-6}$  M to 532 nm at  $2 \times 10^{-4}$  M. The features of the excitation spectrum are also dependent on the concentration. As shown in Figure 1a, below  $1 \times 10^{-5}$  M, there are two absorption peaks at about 315 and 330 nm. The intensity of these peaks increases with increasing concentration, with the maximum intensity at a concentration of  $1 \times 10^{-5}$  M; the

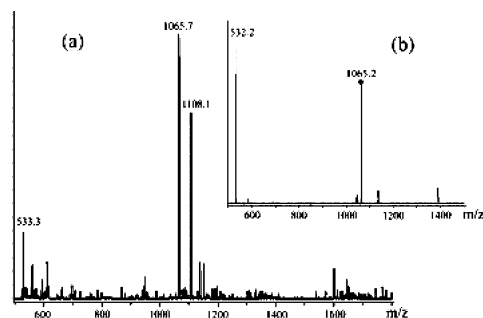


**Figure 2.** (a) Mass spectroscopy of **2** in a DMF solution:  $m/z$  533.3 ( $\text{M}^-$ , calcd  $m/z$  532.5), 1065.7 ( $2\text{M}^-$ ), 1108 [ $2\text{M}^- + \text{N}(\text{CH}_3)_2$ ]. (b) MS/MS spectra of the  $m/z$  1065 fragment;  $m/z$  532.2 ( $\text{M}^-$ , calcd  $m/z$  532.5).

intensity of these peaks then decreases with increasing concentration above this point. However, increasing the concentration above  $2 \times 10^{-5}$  M increases the intensity of two new peaks, at about 270 and 355 nm. At the same time, the intensity of the absorption band around 460 nm continues to increase with increasing concentration (Figure 1b). The concentration-dependent photoluminescence of **2** may be explained by considering the concentration-dependent formation of the  $\pi$ - $\pi$ -stacked dimer in solution. The excitation band between 400 and 500 nm may be ascribed to absorption by a ligand pair. With increasing concentration, the concentration of the ligand pair increases, while the concentration of the ligand monomer decreases, with the stacked ligand pair as the predominant species at concentrations greater than about  $2 \times 10^{-5}$  M. The same phenomenon is apparent in the photoluminescence of **1**, the precursor to **2**, but to a lesser degree.

Further evidence for the existence of the ligand pair in solution comes from mass spectroscopy of **2**, shown in Figure 2. The two peaks visible in Figure 2a at  $m/z$  1065.7 and 533.3 correspond to those of the ligand dimer (calculated  $m/z$  1065) and monomer (calculated  $m/z$  532.5), respectively. The peak of the dimer is verified by MS/MS spectroscopy, shown in Figure 2b, with the signal of the monomer at  $m/z$  532.2. The mass spectroscopy of **1** in an acetone solution also shows the peak of the dimer, indicating that the ligand pair exists not only in the solid state but also within the solution of starting materials.

The pairing of ligands in the solid state is evident from the crystal structure of **3**. As expected from previous studies of *s*-triazine and tri-*s*-triazine found in the literature (vide supra), the structure of HTB in **3** is nearly planar, with prominent  $\pi$ - $\pi$ -stacking effects evident. The crystal structure of **3** shows that the dihedral angle between the phenyl ring and the tri-*s*-triazine plane is only  $6.1^\circ$ . Two ligands are also found stacked together to form a  $D_3$  symmetric ligand pair due to the strong  $\pi$ - $\pi$  interaction between the ligands, as shown in Figure 3; this structure is also found in several *s*-triazine derivatives and named the  $D_3$ -Piedfort unit ( $D_3$ -PU).<sup>13</sup> The rings are aligned through the central nitrogen atoms and rotationally skewed  $22.8^\circ$  about this axis. The distance between the tri-*s*-triazine planes is  $3.328 \text{ \AA}$ , which indicates rather strong face-to-face  $\pi$ - $\pi$  interaction. Similar stacking has also been found in another tri-*s*-triazine derivative, potassium melonate.<sup>5</sup>

(14) (a) Thalladi, V. R.; Boese, R.; Brasselet, S.; Ledoux, I.; Zyss, J.; Jetli, R. K. R.; Desiraju, G. R. *Chem. Commun.* **1999**, 1639. (b) Thalladi, V. R.; Brasselet, S.; Weiss, H.-C.; Blaeser, D.; Katz, A. K.; Carrell, H. L.; Boese, R.; Zyss, J.; Nangia, A.; Desiraju, G. R. *J. Am. Chem. Soc.* **1998**, *120*, 2563.

(15) Schroeder, H.; Kober, E. *J. Org. Chem.* **1962**, *27*, 4262.

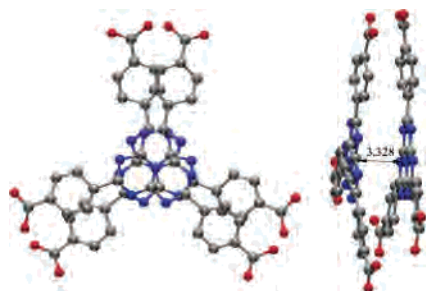


**Figure 3.** Two ligands stacked face-to-face to form a  $D_3$  ligand pair–Piedfort unit ( $D_3$ –PU). Nitrogen atoms are indicated in blue, carbon atoms in gray, oxygen atoms in red, and zinc atoms in aqua.

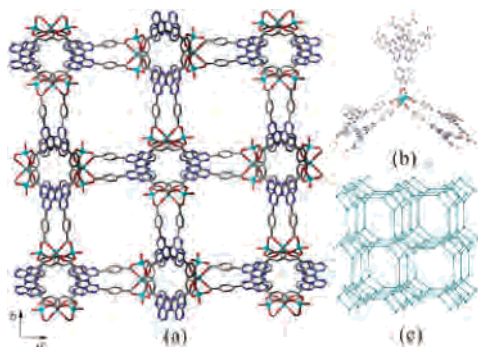


**Figure 4.** (a) Three-dimensional network structure of **3** along the [001] direction. (b) Coordination motif between  $D_3$ –PU ligand pairs and the trinuclear zinc cluster. (c) (10,3)-a network topology of **3**.

The ligand pairs connect through a linear trinuclear zinc cluster to form a three-dimensional framework (Figure 4a). Three zinc atoms are chelated by six carboxylate groups from three  $D_3$ –PU ligand pairs (Figure 4b). The central zinc atom is octahedrally coordinated, while the other two are tetrahedrally coordinated by an oxygen atom from each of the three HTB carboxylate groups and a water molecule.

The connection between  $D_3$ –PU ligand pairs and trinuclear nodes forms a chiral (10,3)-a network. The chiral structure of **3** can be explained by consideration of the assembly of the  $D_3$ –PU pair. The two ligand molecules can stack together in either a clockwise or counterclockwise manner; these two stacking modes are enantiomers. Because all of the ligand pairs in the framework of **3** are clockwise, a chiral network results.

Neutral and noninterpenetrating (10,3)-a networks are highly desired for obtaining chiral high-porosity materials; **3** is a rare example of such a network. Because of the lack of interpenetration and the large ligand size, high porosity can be expected in this MOF: the solvent-accessible volume is 84.4%.<sup>16</sup> This high porosity makes the framework unstable to guest removal: the framework collapses quickly once crystals are removed from the mother liquor, likely because of both the loss of solvent and loss of terminally coordinated water molecules. Thermogravimetric analysis shows that **3** has a weight loss of 24.29% from 30 to 140 °C, corresponding to the loss of free solvent molecules and two coordinated water molecules.

Like other reported tri-*s*-triazine derivatives, **1–3** also have interesting photoluminescence properties. Photoluminescent emission of **1** and **2** was detected at 517 and 532 nm, respectively. A significant shift in the maximum emission is observed when compared to other derivatives of tri-*s*-triazine, for example,  $\lambda_{\text{em}}^{\text{max}}(\text{C}_6\text{N}_7\text{Cl}_3) = 466 \text{ nm}$ ,<sup>7</sup>  $\lambda_{\text{em}}^{\text{max}}[\text{C}_6\text{N}_7(\text{NH}_2)_3] = 366 \text{ nm}$ ,<sup>8</sup>  $\lambda_{\text{em}}^{\text{max}}[\text{C}_6\text{N}_7(\text{N}_3)_3] = 430 \text{ nm}$ ,<sup>10</sup> and  $\lambda_{\text{em}}^{\text{max}}(\text{C}_6\text{N}_7\text{H}_3) = 517 \text{ nm}$ .<sup>11</sup> This result is not surprising because HTB has a considerably larger conjugation system because of the addition of the benzoic acid rings. The solid-state emission spectrum of **3** exhibits a maximum at 391 nm, with a blue shift of about 140 nm from that of the ligand. This can be ascribed to ligand-to-metal charge transfer.

Although a single crystal of **3** is chiral, the bulk sample is a racemic mixture because each of the two enantiomers has an equal chance to crystallize. It may be possible to affect the packing mode of the ligand pair at the beginning of the reaction by adding a chiral structure-directing agent, to favor one enantiomeric dimer over the other, resulting in a crystalline solid that is homochiral in the bulk. Although we do not know the exact packing mode of the dimer in solution, density functional theory calculations can be done to explore various possibilities. Templating studies with this ligand are ongoing in our laboratory, and these results will be reported in future publications.<sup>17</sup>

In conclusion, we have synthesized a tricarboxylate-functionalized ligand based on tri-*s*-triazine and used it to assemble an MOF containing trinuclear zinc clusters. As expected based on the design of the ligand, this MOF was found to be very porous and to possess a noninterpenetrated chiral (10,3)-a network.  $\pi$ – $\pi$  interaction leading to a Piedfort pair of planar HTB ligands was found to be responsible for the formation of the chiral structure. Photoluminescence measurements indicate the existence of the ligand dimer in solution prior to network assembly, and mass spectroscopy corroborates these findings. The existence of the ligand dimer in solution is hoped to provide an exciting opportunity to manipulate, prior to the introduction of the metal center, exactly that piece of the framework that most directly and profoundly affects porosity and stability.

**Acknowledgment.** This work was supported by the National Science Foundation (Grant CHE-0449634), Miami University, and the donors of the American Chemical Society Petroleum Research Fund. We thank Dr. Ian R. Peat for assistance with mass spectroscopy and Michelle A. Smith for synthetic work. H.-C.Z. also acknowledges Research Corporation for a Research Innovation Award and a Cottrell Scholar Award. The diffractometer was funded by NSF Grant EAR-0003201.

**Supporting Information Available:** Experimental procedures and synthetic details for compounds **1–3** and complete crystallographic data (CIF) for compound **3**. This material is available free of charge via the Internet at <http://pubs.acs.org>.

IC051900P

(16) Spek, A. L. *J. Appl. Crystallogr.* **2003**, *36*, 7.

(17) Ma, S.; Sun, D.; Zhou, H.-C., manuscript in preparation, 2006.